Exploring the potential of earthworm gut bacteria for plastic degradation

Davi R. Munhoz, Ke Meng, Lang Wang, Esperanza Huerta Lwanga, Violette Geissen, Paula Harkes

Angaben zur Veröffentlichung / Publication details:

Munhoz, Davi R., Ke Meng, Lang Wang, Esperanza Huerta Lwanga, Violette Geissen, and Paula Harkes. 2024. "Exploring the potential of earthworm gut bacteria for plastic degradation." *Science of The Total Environment* 927: 172175. https://doi.org/10.1016/j.scitotenv.2024.172175.

Science of the Total Environment 927 (2024) 172175

Contents lists available at ScienceDirect

Science of the Total Environment

journal homepage: www.elsevier.com/locate/scitotenv

Exploring the potential of earthworm gut bacteria for plastic degradation

Davi R. Munhoz [a,*,1], Ke Meng [a,1], Lang Wang [a], Esperanza Huerta Lwanga [a,b], Violette Geissen [a], Paula Harkes [a]

[a] Soil Physics and Land Management Group, Wageningen University & Research, Droevendaalsesteeg 3, 6708PB Wageningen, the Netherlands
[b] Agroecología, El Colegio de la Frontera Sur, Unidad Campeche, Av Polígono s/n, Cd. Industrial, Lerma, Campeche, Mexico

HIGHLIGHTS

- *Streptomyces fulvissimus* promoted PLA-f degradation at 30 °C in liquid media.
- Additional carbon source in the liquid media facilitated PLA-f degradation.
- PLA-f degradation triggered a positive correlation between weight loss and pH.
- Strain interplay in the same media could hamper the performance of degraders.
- PLA-f degradation occurred below PLA glass transition temperature.

GRAPHICAL ABSTRACT

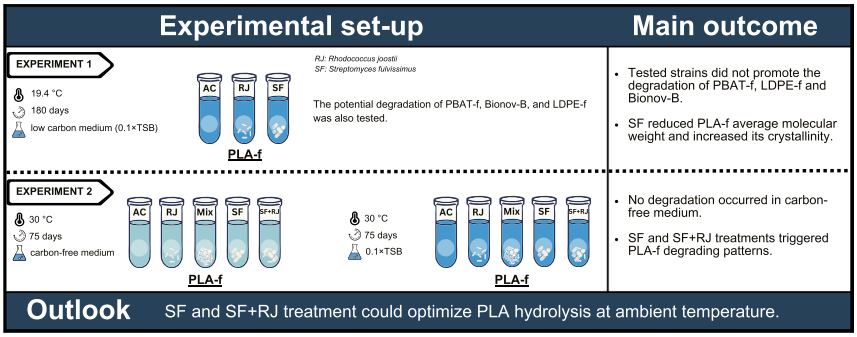

ARTICLE INFO

Editor: Philiswa Nomngongo

Keywords:
Biodegradable mulch films
Biodegradation
Earthworm gut-inhabiting bacterial strains
Polylactic acid (PLA)
Streptomyces fulvissimus

ABSTRACT

The use of plastic mulch films in agriculture leads to the inevitable accumulation of plastic debris in soils. Here, we explored the potential of earthworm gut-inhabiting bacterial strains (*Mycobacterium vanbaalenii* (MV), *Rhodococcus jostii* (RJ), *Streptomyces fulvissimus* (SF), *Bacillus simplex* (BS), and *Sporosarcina globispora* (SG) to degrade plastic films (⌀ = 15 mm) made from commonly used polymers: low-density polyethylene film (LDPE-f), polylactic acid (PLA-f), polybutylene adipate terephthalate film (PBAT-f), and a commercial biodegradable mulch film, Bionov-B® (composed of Mater-Bi, a feedstock with PBAT, PLA and other chemical compounds). A 180-day experiment was conducted at room temperature ($\bar{x}$ =19.4 °C) for different strain–plastic combinations under a low carbon media (0.1× tryptic soy broth). Results showed that the tested strain–plastic combinations did not facilitate the degradation of LDPE-f (treated with RJ and SF), PBAT-f (treated with BS and SG), and Bionov-B (treated with BS, MV, and SG). However, incubating PLA-f with SF triggered a reduction in the molecular weights and an increase in crystallinity. Therefore, we used PLA-f as model plastic to study the influence of temperature ("room temperature" & "30 °C"), carbon source ("carbon-free" & "low carbon supply"), and strain interactions ("single strains" & "strain mixtures") on PLA degradation. SF and SF + RJ treatments significantly fostered PLA degradation under 30 °C in a low-carbon media. PLA-f did not show any degradation in carbon-free media treatments. The competition between different strains in the same system likely hindered the performance of PLA-degrading strains. A positive correlation between the final pH of culture media and PLA-f weight loss was observed, which might reflect the pH-dependent hydrolysis mechanism of PLA. Our results situate SF and its co-

* Corresponding author at: Droevendaalsesteeg 3, 6708PB Wageningen, the Netherlands.
E-mail address: davi.munhoz@wur.nl (D.R. Munhoz).
[1] The authors contributed equally.

https://doi.org/10.1016/j.scitotenv.2024.172175
Received 15 January 2024; Received in revised form 21 March 2024; Accepted 1 April 2024
Available online 2 April 2024

culture with RJ strains as possible accelerators of PLA degradation in temperatures below PLA glass transition temperature (T_g). Further studies are needed to test the bioremediation feasibility in soils.

1. Introduction

Agricultural soils play a vital role in supporting food production and sustaining ecosystem services and have become repositories for plastic waste originating from diverse sources. Notably, agricultural practices, such as plastic mulching for weed control and moisture retention, have been identified as contributors to plastic pollution in agricultural soils (Sa'adu and Farsang, 2023). The accumulation of plastic presents risks to soil health, crop productivity, and the overall sustainability of agricultural systems (Rillig et al., 2017; Rillig et al., 2019).

Low-density polyethylene (LDPE) based mulch films have been widely used in agricultural production for their excellent material properties but are difficult to recover by the end of the crop season (Liu et al., 2014). The residuals can fragmentize into smaller debris and accumulate in the soil due to LDPE's inert chemical properties (Khalid et al., 2023). Alternative mulch films, produced with biodegradable polymers and designed to degrade in the soil, appear as potential substitutes for the LDPE mulch films. Polylactic acid (PLA) and polybutylene adipate-*co*-terephthalate (PBAT) and their blends have become popular options among other materials (e.g., starch, cellulose, vegetable oils, etc.) to replace LDPE mulch in agricultural soils. For example, Mater-Bi, Bionov-B®, and others. The ratio of PLA content in the blend is often around 3–20 % for mulch films and could reach even 40 % for seedling trays (Meng et al., 2023a). The biodegradability of PBAT under controlled conditions has been demonstrated (Zumstein et al., 2019); however, polymer degradation depends not just on the polymer's biodegradability but also on the soil characteristics, availability of microbial degraders, environmental conditions, among other factors (Sander, 2019; Han et al., 2021). That is why some studies have also reported slow degradation of biodegradable plastics when the testing conditions are different or not optimal (Sintim et al., 2020; Griffin-LaHue et al., 2022; Meng et al., 2023a). Therefore, the potential accumulation of biodegradable mulch films in the soil should also be taken seriously.

Currently, the prevailing strategies for managing plastic waste are incineration and landfills (Chen et al., 2021). However, these methods may not be suitable for dealing with plastic-contaminated soils where separating plastic residues from the sites is difficult, if not impossible. The in-situ bioremediation strategy, which exhibits advantages such as low energy cost and eco-friendliness, is worth exploring as a potential option for dealing with microplastic-contaminated soils.

Bacteria in the soil and the gut of some insects have shown the potential to biodegrade certain plastics (Yang et al., 2014; Yoshida et al., 2016). The aptitude of certain microorganisms to tackle biodegradable plastics, including PLA and PBAT, has uncovered promising results. For instance, *Bacillus* sp. *JY35* isolated from soil (sludge) specimens, demonstrated the capacity to catalyze the degradation of PBAT and PLA following a brief incubation within a liquid medium. This process induced perceptible alterations in the physicochemical attributes of the plastics (Cho et al., 2022). *Bacillus safensis* isolated from landfill soil showed the potential to utilize PLA as the sole carbon source at 30 °C (Wang et al., 2023). Wufuer et al. (2022) reported that *Peribacillus frigoritolerans S2313* could target amorphous regions in PBAT and carry out biodegradation by a speculated oxidative process. Although research has shown the involvement of gut bacteria sourced from *Zophobas atratus* in enhancing LDPE degradation (Peng et al., 2020), comprehensive evidence substantiating the potential efficacy of bacterial degradation in the context of LDPE remains limited.

The biodegradation of plastic can be affected by many factors besides the biodegradability of the polymers per se (Chamas et al., 2020). PLA degradation has been reported as faster under higher temperatures, a pattern verified for PLA films from different providers (Ho et al., 1999). Nutrient availability is another factor capable of affecting biodegradation. Bonifer et al. (2019) have found that additional phosphate and potassium hindered the PLA degradation by *Bacillus pumilus* (*B12*) while adding specific carbon sources facilitated the process. For instance, soytone has shown the potential to enhance PLA biodegradation compared to other nitrogen sources or no nitrogen source conditions (Boonluksiri et al., 2021). Therefore, temperature and nutrient availability should be investigated to enhance the understanding of the potential of bacteria in plastic degradation.

Reduced recovery of LDPE microplastics was reported in sterile sandy soil inoculated with bacterial strains isolated from the gut of *Lumbricus terrestris* (Huerta Lwanga et al., 2018). Moreover, we conducted a pilot experiment in 2022 (Table S6) in which two combinations of these bacteria showed high degradation potential for PLA films at 30 °C after 180 days, suggesting a potential broader use of earthworm gut bacteria to optimize PLA degradation under temperatures below its glass transition temperature (T_g). In addition, recent studies also reported that PLA and PBAT microplastics could undergo slight depolymerization inside the gut of *Lumbricus terrestris* (Meng et al., 2023a, 2023b; Adhikari et al., 2023). Therefore, studying these earthworm gut-inhabiting strains as plastic bioremediation candidates is of great scientific interest.

In this study, we investigated the potential of *Streptomyces fulvissimus*, *Rhodococcus josti*, *Mycobacterium vanbaalenii*, *Bacillus simplex*, and *Sporosarcina globispora* to degrade plastic films used in agriculture, that is, a conventional LDPE film (LDPE-f) and other films promoted as biodegradable, such as PLA film (PLA-f), PBAT film (PBAT-f) and a commercial film mainly comprised of a PBAT–PLA blend (Bionov-B). These biodegradable plastics are proven to degrade under lab conditions but not necessarily under agricultural practices. Furthermore, we used PLA film (⌀ = 15 mm, 50 μm thickness) as a model to study the effect of strain mixture, temperature, and carbon supply on PLA biodegradation.

2. Materials and methods

2.1. Bacterial strains and culture media

2.1.1. Bacterial strains

Five bacterial strains isolated from the gut of *Lumbricus terrestris* in a previous study (Huerta Lwanga et al., 2018) have shown the potential for the degradation of certain plastics in a preliminary pilot test (Table S6). Therefore, the following strains classified as Actinobacteria were tested in this research, more specifically *Mycobacterium vanbaalenii* (Fig. S1), *Rhodococcus jostii* (Fig. S2) and *Streptomyces fulvissimus* (Fig. S3), together with the strains belonging to the Firmicutes (recently named as Bacillota) phylum, i.e., *Bacillus simplex* (Fig. S4) and *Sporosarcina globispora* (Fig. S5). These strains were stored in glycerin in a deep freezer (−80 °C) after being isolated from the gut. Before the start of this research, the strains were revived on tryptic soy broth (TSB) agar plates and preserved at 4 °C.

2.1.2. Culture media and buffers

A low-carbon medium: 0.1× TSB liquid medium (Oxoid Ltd., England) and a carbon-free (CF) liquid medium were used in the experiments. The 0.1× TSB medium was composed of 3.0 g TSB powder per liter of demineralized water (10 times diluted TSB), while the CF medium contained 0.7 g KH_2PO_4, 0.917 g $K_2PO_4{\cdot}3H_2O$ 1.0 g NH_4NO_3, 0.005 g NaCl, 0.002 g $FeSO_4{\cdot}7H_2O$, 0.002 g $ZnSO_4{\cdot}7H_2O$, 0.001 g $MnSO_4{\cdot}7H_2O$, and 0.7 g $MgSO_4{\cdot}7H_2O$ per liter of demineralized water, with pH adjusted to 7.0. Both media were autoclaved at 121 °C and

under 0.15 MPa air pressure. The 0.1× TSB agar plates were prepared with 1.5 % (*w/v*) agar powder in the liquid medium. Phosphate buffer saline (PBS) was prepared following the formula (in 1 L): 8.00 g NaCl, 0.20 g KCl, 1.44 g Na_2HPO_4 and 0.24 g KH_2PO_4 with pH adjusted to 7.4. The pH of all solutions was adjusted with 0.1 M HCl or 0.1 M NaOH solutions using pH indicator paper sticks (6.0–7.7).

2.2. Plastics films

We tested four types of plastic films in this study, which are a PBAT film (ca. 50 μm, ecoflex® F Blend C1200, BASF), a PLA film (ca. 50 μm, NatureWorks® Biopolymer 2003D), a commercial biodegradable mulch film (Bionov-B®, foil class B, ca. 15 μm, 3.2 % PLA- + 71.3 % PBAT-based, containing unquantified starch, plasticizers, and inorganic fillers) and a LDPE film (made by blow molding (15–20 μm) at Axis, Wageningen University and Research, the Netherlands). Bionov-B contains additives, but we could not gather any information on their chemical composition. To facilitate the reading process, we henceforth abbreviate the plastic films as PBAT-f, PLA-f, LDPE-f, and Bionov-B. Further information on the polymers can be found in Table S1. Prior to use, they were cut into small disks (Φ = 1.5 cm), soaked in 70 % ethanol solution for 20 min, disinfected under UV light for 30 min (UVC 254 nm, 40 W), and air-dried overnight in the biosafety cabinet.

2.3. Experimental design

2.3.1. Experiment 1

Experiment 1 is a 180-day incubation experiment carried out in test tubes at room temperature ($\bar{x}$ =19.4 °C). The experiment intended to explore the potential of different bacterial strains to facilitate plastic degradation under conditions less optimal for bacterial growth but representative of environmental conditions. Nine treatments (plastic–-strain combinations, three replicates) and four abiotic controls (AC, incubation without strains) with five replicates were established based on the results of our pilot test. Specifically, *S. fulvissimus* (SF) and *R. jostii* (RJ) were considered potential degraders for PLA-f and LDPE-f, *B. simplex* (BS) and *S. globispora* (SG) were applied to degrade PBAT-f and Bionov-B. Moreover, *M. vanbaalenii* (MV) was also tested as a candidate to facilitate Bionov-B degradation (Table 1). The temperature was recorded by a datalogger per 15 min (CAMPBELL SCIENTIFIC CR1000) and ranged from 10 to 32 °C (average 19.4 ± 4.3 °C) throughout the experiment (Fig. S6).

We started the experiment by transferring single colonies from the agar plates into 50 mL of sterile 0.1× TSB medium in an Erlenmeyer flask (100 mL). After incubation overnight (150 rpm, 30 °C), the OD600 values were measured with Nanodrop One (Thermo Fisher Scientific Inc.). The cell concentrations of the inocula were adjusted to similar levels (in terms of CFU/mL) by concentrating/diluting the cell suspensions based on established OD600–CFU/mL curves (Fig. S7). That step was not conducted for SF and MV because we did not set their OD600–CFU/mL curve. The cell aggregations of SF and MV have led to variances in their OD600 measurements. The concentrations of SF and MV inocula were quantified by spread plating instead. Detailed information on inoculum concentrations can be found in Text S1 and Table S2. After concentrating/diluting the inocula, 1 mL was transferred into a test tube containing 9 mL sterilized 0.1× TSB medium. Four plastic film disks were weighed together and added into each tube with sterile tweezers. The test tubes were shaken at 130 rpm at room temperature in the dark to avoid potential photodegradation. AC treatment was sampled only after 180 days, while treatments inoculated with strains after 90 days and 180 days. We did not supply additional fresh medium during the incubation because we hoped to reduce the potential contamination and verify if the test strains would be able to utilize the plastic films in the long term.

Furthermore, to help visually inspect the colonization of tested strains on different plastic films, we performed another plastic incubation on 0.1× TSB agar plates. Briefly, after centrifuging the overnight incubated cell cultures at 3500 rpm for 15 min, the supernatants were discarded, and the cell pellets were re-suspended with 20 mL 1× PBS solution (pH 7.4) in the Falcon tubes. This step was to harvest and wash cells from the 0.1× TSB liquid medium. Then 50 μL cell suspension was spread-plated on the agar plates. Finally, one plastic disk per plastic type (totaling four) was carefully placed on top of the media using a sterilized metal tweezer. All agar plates were sealed with parafilm and stored upside down at room temperature in the dark for 180 days.

2.3.2. Experiment 2

This experiment scaffolded in Experiment 1, aimed to enhance our understanding of how carbon source availability, inter-species interaction, and temperature would affect PLA-f degradation. Ten treatments were established at 30 °C for 75 days (Table S3). PLA-f (⌀ = 15 mm, 50 μm thickness) was incubated in abiotic control (AC), and with *S. fulvissimus* (SF), *R. josti* (RJ), *S. fulvissimus* + *R. jostii* (SF + RJ), and a mixture of all strains (*S. fulvissimus* + *R. jostii* + *B. simplex* + *S. globispora* + *M. vanbaalenii*) (Mix) in 0.1× TSB and CF liquid media, respectively. The microorganisms were transferred from a single colony and inoculated in a test tube with 10 mL culture media. These tubes were sealed with rubber stoppers, shaken at 150 rpm, and opened twice weekly in a biosafety cabinet to ensure aeration.

Table 1
Nine treatments and four abiotic controls were established in 0.1× TSB liquid culture media incubated at room temperature ($\bar{x}$ =19.4 °C) within two periods (90 and 180 days).

Plastic	Treatment	Initial cell concentration (CFU/mL)
PBAT-f	Abiotic control (AC)	0
	B. simplex (BS)	~2×10^6
	S. globispora (SG)	~2×10^6
PLA-f	Abiotic control (AC)	0
	S. fulvissimus (SF)	~3.3×10^3
	R. jostii (RJ)	~2×10^6
Bionov-B	Abiotic control (AC)	0
	B. simplex (BS)	~2×10^6
	S. globispora (SG)	~2×10^6
	M. vanbaalenii (MV)	~1.1×10^6
LDPE-f	Abiotic control (AC)	0
	S. fulvissimus (SF)	~3.3×10^3
	R. jostii (RJ)	~2×10^6

2.4. Plastic sampling and cleaning

By the end of the experiment, plastic disks were collected with sterile tweezers, and the remaining culture media was transferred into sterile centrifuge tubes (15 mL). All plastic disks underwent a cleaning procedure except for those designated for scanning electron microscopy (SEM) analysis. The cleaning procedure was as follows: collected plastic disks were rinsed with demineralized water, followed by ultrasonication for 30 min in a 10 mL sodium dodecyl sulfate solution (SDS, 2 % *w/v*). The SDS solution was subsequently rinsed from the disks, which were then immersed in 45 mL of demineralized water and subjected to ultrasonic bathing for an hour. The disks were thoroughly rinsed again with demineralized water, and the remaining biofilm on the surface (if any) was gently removed. Finally, the disks were placed in a glass tube containing 70 % ethanol and left to dry overnight in an oven at 40 °C.

2.5. Characterization of plastic degradation

2.5.1. pH of the liquid media

The main degradation mechanism of PLA and PBAT is hydrolysis, which can be affected by and lead to changes in pH. Therefore, the liquid media pH value was measured at the beginning and end of the experiment with a pH meter (Fisher Scientific®, Fisherbrand accumet FE150®, The Netherlands).

2.5.2. Weight loss

The following calculation was carried out for each replicate to measure gravimetric weight loss:

$$Weight\ Loss\ (\%) = \left(\frac{m_{int} - m}{m_{int}}\right) \times 100$$

where: m_{int} (g) is the dry weight of plastic disks measured before the experiment, and m (g) is the dry weight of disks after 180 days measured after cleaning procedures.

2.5.3. Characterization of the chemical composition

Fourier transform infrared (FTIR) spectroscopy equipped with an attenuated total reflectance (ATR) accessory (Cary 630 FTIR) was used to characterize the chemical composition of the plastic disks. Spectral acquisition was conducted within the range of 650–4000 cm^{-1}, with 32 background scans and 64 sampling scans at a resolution of 2 cm^{-1}. Obtained spectra were auto-smoothened and baseline-corrected with EZ OMNIC.

To profile the changes in LDPE-f chemical composition after bacterial treatments, the carbonyl index (CI) was calculated as follows:

$$CI = \frac{\text{Area under band from 1650–1800 cm}^{-1}}{\text{Area under band from 1420–1500 cm}^{-1}}$$

where the area under the band from 1650 to 1800 cm^{-1} represents the area of carbonyl (C=O), and the area under the band from 1420 to 1500 cm^{-1} represents the area of methylene (CH_2).

The CI value adds value to the biodegradation discussion since LDPE plastics that are more degraded tend to have higher CI. Oxidation is one of the key processes triggering LDPE degradation and C=O formation. When comparing the CI of a degraded LDPE and a pristine LDPE, the latter will show lower CI due to the lack of C=O and their solid C—H backbone and stable CH_2 bonds (Fig. S12).

2.5.4. Determination of the molecular weight distributions of PLA-f and PBAT-f

For PBAT-f and PLA-f, we selected treatments showing significant weight loss compared to AC from both experiments for GPC analysis. Pristine samples and samples in AC were also measured for comparison. The GPC analysis was conducted using an OmniSEC Reveal GPC system equipped with an OmniSEC Resolve Triple Detector Array (comprising RALLS and LALLS light scattering detectors, a refractive index detector, and a viscometer detector). The specific effluent selected for the experiment was 1,1,1,3,3,3-hexafluor-2-propanol (HFIP) with 0.02 M KTFA, and it was delivered at a flow rate of 0.7 mL/min. The GPC columns employed were a PSS PFG analytical linear M column and a guard column, suitable for the molecular range of approximately 300–2 × 10^6 Da (PMMA in HFIP), and the column oven was maintained at 35 °C.

Weighed polymer samples were dissolved overnight in 3 mL of the selected effluent within 4 mL GLC vials. The polymer concentrations were adjusted to be between 3 and 4 mg/mL in the liquid phase of the samples. Before measurement, the samples were filtered using 0.45 μm PTFE syringe filters. The standard injection volume was 100 μL for each one. Weight-average molecular weight (M_w), number-average molecular weight (M_n), *Z*-average molecular weight (M_z), and polydispersity index (PDI = M_m/M_n) were determined based on the measured molecular weight distributions (MWDs). All measurements were carried out in duplicate to ensure precision and accuracy. For absolute calibration of the system, we used a narrow standard PolyCAL PMMA 50kD (from Viscotek) (M_w = 49,697 Da; PDI= 1.032; W_t= 21.50 mg/10 mL eluent).

2.5.5. Thermodynamic properties of PBAT-f and PLA-f

The thermodynamic properties of PBAT-f and PLA-f samples subjected to GPC analysis were also characterized by differential scanning calorimetry (DSC). The analysis was conducted following ISO 11357 standards using a Perkin Elmer DSC 8000 instrument equipped with a liquid nitrogen cooling system for rapid cooling. Stainless steel cups with a capacity of 60 μL were utilized to contain the sample and serve as reference materials for calibration. The samples were used in their original state and carefully placed within a stainless-steel cup before being hermetically sealed. They were held for 2 min at 0 °C and then heated to 200 °C at 10 °C/min. The degree of crystallinity χ was calculated as (Maaskant et al., 2023):

$$\chi = \frac{\Delta H_m - \Delta H_{cc}}{\Delta H_0}$$

where ΔH_m is the enthalpy change (J/g) during the melting event, ΔH_{cc} is the enthalpy change during the cold crystallization, and ΔH_0 represents the melting enthalpy change of a 100 % crystallized material. ΔH_0 equals 93 J/g (Zhang et al., 2018) for PLA and 114 J/g for PBAT (Tsou et al., 2022).

2.5.6. Microbial colonization and surface morphological changes

Surface morphological changes of the plastics, selected after visual inspection and weight loss measurements for Experiment 1 and 2, were analyzed by SEM at the Wageningen Electron Microscopy Center, the Netherlands. The microorganisms present on the plastisphere were immobilized using 2.5 % (*v*/v) glutaraldehyde (Agar Scientific, Wetzlar, Germany) dissolved in 0.1 M PBS. Subsequently, the samples underwent a series of treatments, i.e., PBS rinse for 15 min, gradual dehydration using an increasing ethanol concentration sequence (30 %, 50 %, 70 %, 90 %, 96 %, and 100 %) for 5 min each, with the final step repeated twice for 10 min each. Plastic samples containing plastisphere microorganisms were subjected to critical point drying using liquid CO_2 (Polaron, GaLa Instrumente, Bad Schwalbach, Germany), followed by immersion in 100 % ethanol and coated with a 12-nm layer of tungsten/iridium using a Sputter Coater (EM SCD500, Leica, Wetzlar, Germany). The coated samples were then examined using a scanning electron microscope (FEI Magellan 400Hitachi S-4800, Oregon, United States) operating at a 2000-kV acceleration voltage and 13pA within a high vacuum environment. SEM images zoomed in on the surface morphology and colonization of different strains for LDPE-f, Bionov-B, PBAT-f, and PLA-f incubated on a 0.1× TSB agar plate under room temperature (19.4 °C) after 180 days (Experiment 1). SEM micrographs were also taken for PLA-f from Experiment 2, incubated for 75 days at 30 °C in 0.1 x TSB liquid culture media with and without the presence of SF, RJ, and SF + RJ.

2.6. Statistical analyses and visualization

All statistical analyses were conducted using R version 4.3.1. The assumptions of normal distribution and equal variance were verified for all measurements using the Shapiro-Wilk test and Levene's test from the "car" package. For data meeting these assumptions, pair comparisons were performed using the *t*-test, while multiple group comparisons were conducted using one-way ANOVA followed by Tukey's post-hoc test. If the data did not meet the normality and equal variance assumptions, pair comparisons were carried out using the Mann-Whitney *U* test, and multiple group comparisons were conducted using the one-way Kruskal–Wallis test, followed by Dunn's test for post-hoc analysis. The significance level was set as $\alpha = 0.05$.

3. Results

3.1. Weight loss

LDPE-f lacked any observable weight loss in any treatment throughout the 180-day incubation (Fig. 1A). PBAT-f exhibited a weight loss of 0.78 ± 0.07 % over 180 days when exposed to the SG treatment, which was significantly higher than the AC treatment (0.53 ± 0.11 %) and the BS treatment (0.58 ± 0.07 %) ($p < 0.05$, Fig. 1B). The weight

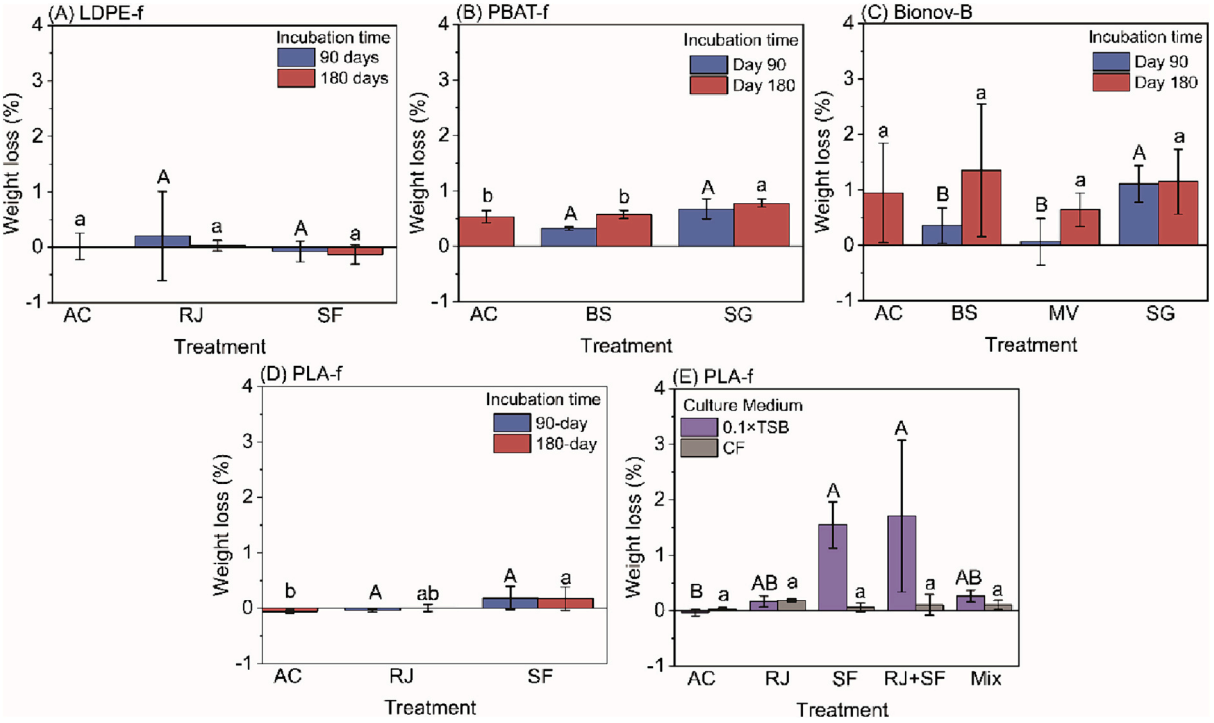

Fig. 1. (A-D) Weight loss of plastic films under room temperature ($\bar{x}$ =19.4 °C) in Experiment 1. Significant differences in the weight loss between treatments in 90 days and 180 days were labeled with uppercase and lowercase letters, respectively (one-way ANOVA). (E). Weight loss of PLA-f at 30 °C in Experiment 2. Significant differences in the weight loss between treatments in 0.1× tryptic soy broth medium (0.1 × TSB) were labeled with uppercase letters. Significant differences in the weight loss between treatments in carbon-free medium (CF) were labeled with lowercase letters (one-way ANOVA). Error bars represent standard deviations (n = 3–5). AC: abiotic control; RJ: *R. jostii*; SF: *S. fulvissimus*; RJ + SF: mixture of SF and RJ; BS: *B. simplex*; SG: *S. globispora*; MV: *M. vanbaalenii*; Mix: mixture of all strains.

loss of PBAT-f in SG and BS did not show an evident increase with the extension of incubation time (from 90 days to 180 days). PLA-f had a weight loss of 0.17 ± 0.21 % ($p < 0.05$) in the SF treatment after 180 days, while the AC (−0.06 ± 0.03 %) and the RJ treatment (0.01 ± 0.06 %) yielded no weight loss (Fig. 1D). No significant difference was observed between the weight loss of Bionov-B in AC, BS, MV, and SG after 180 days of incubation under room temperature ($p > 0.05$, Fig. 1C). Although statistical significance was reached for some inter-treatment comparisons, the influence of selected strains on plastic weight loss was negligible due to the minimal absolute difference in weight loss between treatments.

Interestingly, the influence of some strains on PLA-f weight loss became evident under elevated temperatures (30 °C). Preeminent weight losses of PLA-f were found with the presence of SF (1.55 ± 0.41 %) and SF + RJ (1.71 ± 1.37 %), compared with the control (−0.03 ± 0.06 %) ($p < 0.05$, Fig. 1E). PLA-f incubated in 0.1× TSB with RJ or Mix also showed no weight loss differences compared to the control ($p > 0.05$). While using carbon-free media, i.e., without additional carbon sources, none of the treatments showed any effect on the PLA-f weight loss (Fig. 1E).

3.2. Changes in the chemical composition

ATR-FTIR data did not show significant changes regarding chemical composition for any of the studied plastics after 180 days (Figs. S8–S11).

The CI values displayed subtle fluctuations under different treatments, where the values in SF were the lowest (90 days: 0.28 ± 0.16; 180 days: 0.23 ± 0.18), followed by the ones in RJ (90 days: 0.32 ± 0.06; 180 days: 0.32 ± 0.13. Nevertheless, such changes in CI did not reach statistical significance ($p > 0.05$). In Experiment 2, the only observable difference in the IR spectra of PLA-f was among the treatments in CF. A broad peak occurred within the 3200–3600 cm^{-1} range for PLA-f in RJ, a pattern indicating the hydroxyl stretching or fixed hydrogen bond (Fig. S13). However, such a difference did not occur in all samples recovered from the same treatment. Therefore, we do not consider it a significant change in the functional groups.

3.3. Molecular weight changes

Compared to the pristine PLA-f, PLA-f in AC treatment showed little change in the M_n, M_w, and M_z after incubation at room temperature for 180 days. Notably, in the presence of SF, the M_n, M_w, and M_z of PLA-f decreased by 18.3 %, 16.2 %, and 19.6 % compared to AC (Fig. 2B, Table S4). The PLA-f PDIs were not significantly affected by the treatments (range 1.96–2.01), which is also supported by the molecular weight distribution curves (Fig. S14). Compared to pristine PBAT-f, PBAT-f under AC treatment showed higher M_n (+20.0 %) and lower M_z (−12.6 %) after 180 days of incubation (Fig. 2A). However, we did not find an evident difference between PBAT-f molecular weights (M_n, M_w, and M_z) in AC and SG. The PDI of pristine PBAT-f was 2.93, higher than PBAT-f in AC (2.36) and SG (2.56). Similar trends can also be found in their molecular weight distribution (Fig. S14).

For PLA-f incubated at 30 °C (Experiment 2), the molecular weights (M_n, M_w, M_z) of PLA-f in AC, SF, and SF + RJ all decreased by at ca. 30 % compared to the pristine, but the differences between AC, SF, and SF-RJ were negligible (Fig. 2C & Table S4). The PDIs of PLA-f in AC, SF, and SF + RJ ranged between 1.81 and 1.90, slightly lower than the pristine sample (2.01). The shift of molecular weight distributions of incubated samples compared to the pristine sample was also evident (Fig. S15).

3.4. Changes in PLA-f and PBAT-f thermodynamic properties

The DSC curves of measured samples are displayed in Table S5. Pristine PLA-f was almost completely amorphous (ΔH_m 0 J/g, DSC crystallinity 0 %). The absolute value of enthalpy change associated with cold crystallization was about the same as the melting enthalpy.

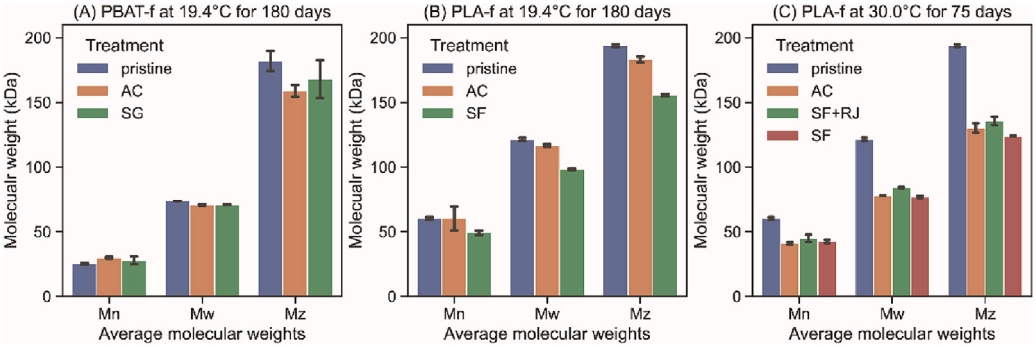

Fig. 2. Changes in the molecular weight of PBAT-f and PLA-f after exposure to different strains. (A). Pristine PBAT-f and PBAT-f (AC and SG) for 180 days at room temperature ($\bar{x}$ =19.4 °C). (B). Pristine PLA-f and PLA-f (AC and SF) at room temperature ($\bar{x}$ =19.4 °C) for 180 days. (C) Pristine PLA-f and PLA-f (AC, SF-RJ, and SF) at 30 °C for 75 days. Error bars are standard deviations calculated from duplicate measurements on the same sample. Mn: number average molecular weight; Mw: weight average molecular weight; Mz: *Z*-average molecular weight. AC: abiotic control; SF: *S. fulvissimus*; SF + RJ: mixture of SF and RJ; SG: *S. globispora*.

Discrepancies in thermodynamic properties were observed in PLA-f samples incubated for 180 days (Table 2). Whereas PLA-f samples in all other treatments were amorphous, PLA-f subjected to SF treatment was almost completely crystalline (ΔH_m 27.5 J/g, DSC crystallinity 30 %), showing almost no cold crystallization. However, the PLA-f exposed to SF in Experiment 2 did not show a significant change in these indicators. For PBAT-f, samples in different treatments did not show significant differences in melting temperature and ΔH_m.

3.5. Plastic morphology and bacterial colonization

SEM was conducted on plastic disks attached to a TSB agar plate containing SF. Notably, both PLA-f and Bionov-B exhibited a substantial development of biofilm, with this phenomenon being particularly conspicuous in the case of the Bionov-B samples. In contrast, the surfaces of PBAT-f and LDPE-f samples displayed minimal signs of biofilm formation. This disparity in biofilm development among the Bionov-B, PLA-f, PBAT-f, and LDPE-f potentially underscores the influence of material composition and physicochemical properties on biofilm adhesion and growth (Fig. 3).

The micrographs indicate biofilm formation on the PLA-f surface after being incubated with different strains (Fig. 4). No obvious biofilm was found on the surface PLA-f in AC. SF + RJ treatment had the densest biofilm formation followed by SF and RJ treatments, respectively.

3.6. Changes in liquid media pH

The pH values of culture media (0.1× TSB) under AC after 180 days showed some treatment-dependent difference. The pH of LDPE-f (8.50 ± 0.14) was significantly higher than PLA-f, PBAT-f, and Bionov-B® ($p \leq 0.05$). Variations in pH were observed in the culture media with LDPE-f and PLA-f (Fig. S16). Specifically, the presence of SF and LDPE-f led to a higher culture media pH of 8.60 ± 0.05 ($p < 0.05$) compared to the counterpart inoculated with RJ, which exhibited a pH of 8.21 ± 0.13 after 90 incubation days. This distinction stood out ($p < 0.05$) after 180 days, with the pH from SF increasing to 8.73 ± 0.03, while the one from RJ treatment decreased to 7.71 ± 0.27. Similarly, the pH increased in the SF-inoculated culture media with PLA-f after 180 days. In particular, the culture media pH values containing SF and PLA were 8.42 ± 0.05 ($p < 0.05$), surpassing the control condition at 8.01 ± 0.25 and the RJ treatment at 7.86 ± 0.09. For both Bionov-B and PBAT-f, the pH values were higher when incubated for 180 days than 90 days in the culture media (Fig. S16). However, the differences were not significant ($p > 0.05$).

Moreover, we observed a positive correlation between the observed weight loss in plastic materials and the corresponding pH levels. This trend was particularly evident for PBAT-f (Fig. S16), where higher weight loss always aligned with elevated pH levels ($p \leq 0.05$). Furthermore, the presence of SG consistently coincided with higher pH values (Figs. S16–17), suggesting that the presence of SG potentially contributed to the pH increase in its immediate environment, thus promoting PBAT-f degradation in terms of weight loss.

To deepen the understanding of PLA-f degradation, we also carried out a linear least-squares regression between the pH of culture media and the PLA-f weight loss after 75 days of incubation (Experiment 2, Fig. 5). Substantial changes in pH were observed in both the CF and 0.1× TSB liquid culture media. The Mix treatment in CF media had a significantly reduced pH (6.69 ± 0.01) compared to the control (6.90 ± 0.01) ($p \leq 0.05$). In 0.1× TSB media, all treatments had significantly elevated pH levels compared to the abiotic control (7.16 ± 0.05) ($p \leq 0.05$). Treatments incubated with SF (SF, SF, RJ, Mix) were consistently correlated with higher pH values (SF: 7.70 ± 0.06, SF + RJ: 7.61 ± 0.07, Mix: 7.64 ± 0.08), followed by the RJ treatment (7.34 ± 0.04).

Table 2
Glass transition temperature (T_g), crystallization temperature (T_c), melting temperature (T_m), and the melting enthalpy (ΔH_m) of PLA-f and PBAT-f. Pristine PLA-f and PBAT-f samples without any treatment were also measured as references. AC: abiotic control; RJ: *R. jostii*; SF: *S. fulvissimus*; SG: *S. globispora*.

Plastic	Incubation time (d)	Incubation temp (°C)	Treatment	Tg (°C)	T_c (°C)	T_m (°C)	ΔH_m (J/g)
PLA-f	N.A.	N.A.	Pristine	58.5	120.5	153.7	0.0
	180	19.4	AC	59.1	116.4	155.0	0.0
	180	19.4	SF	59.1	92.9	153.4	27.5
	75	30	AC	58.0	110.9	154.0	1.1
	75	30	SF + RJ	59.3	112.4	148.7	0.0
	75	30	SF	58.9	112.7	154.9	0.0
PBAT-f	N.A.	N.A.	Pristine	N.A.	N.A.	53.5, 119.9	17.3
	180	19.4	AC	N.A.	N.A.	65.6, 120.8	16.5
	180	19.4	SG	N.A.	N.A.	65.6, 125.6	16.9

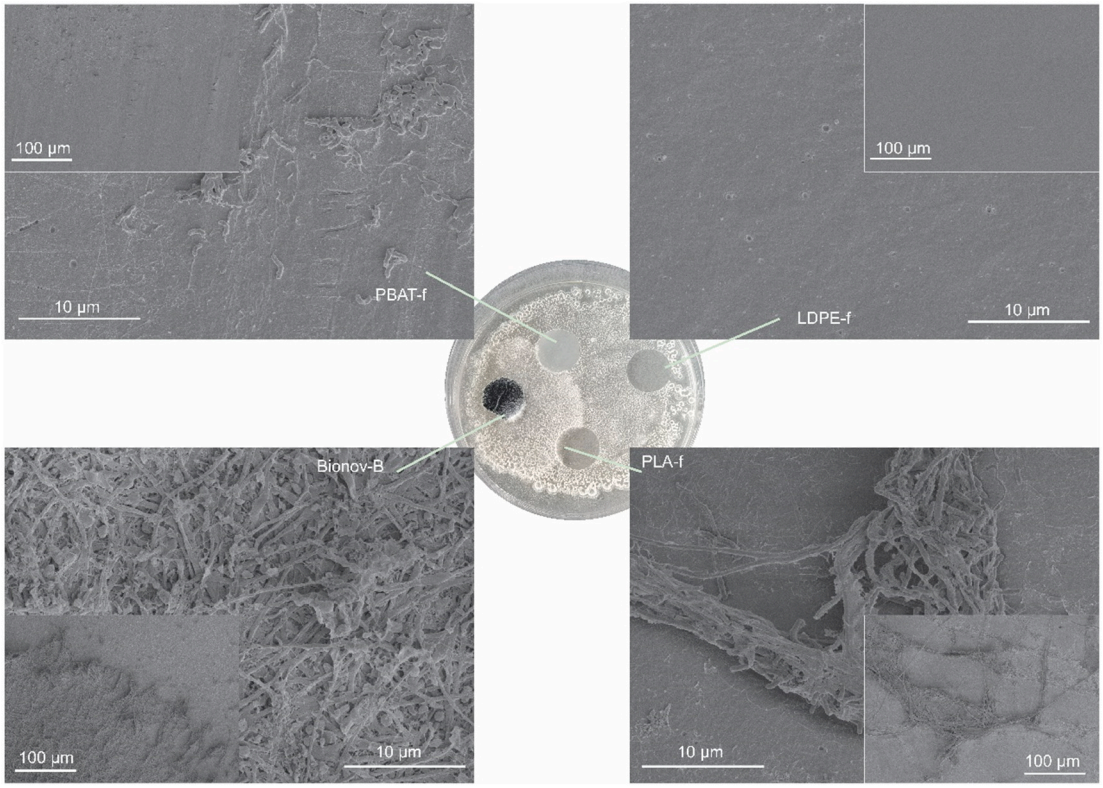

Fig. 3. Petri dish photo portraying the colonization and growth of *S. fulvissimus* on different plastic films on a 0.1× TSB agar plate (central image) under room temperature (19.4 °C) after 180 days. Corresponding scanning electron microscope (SEM) images taken under 5000× and 500× (inset picture) magnifications exhibit the surface morphology and colonization of *S. fulvissimus* on different plastic films.

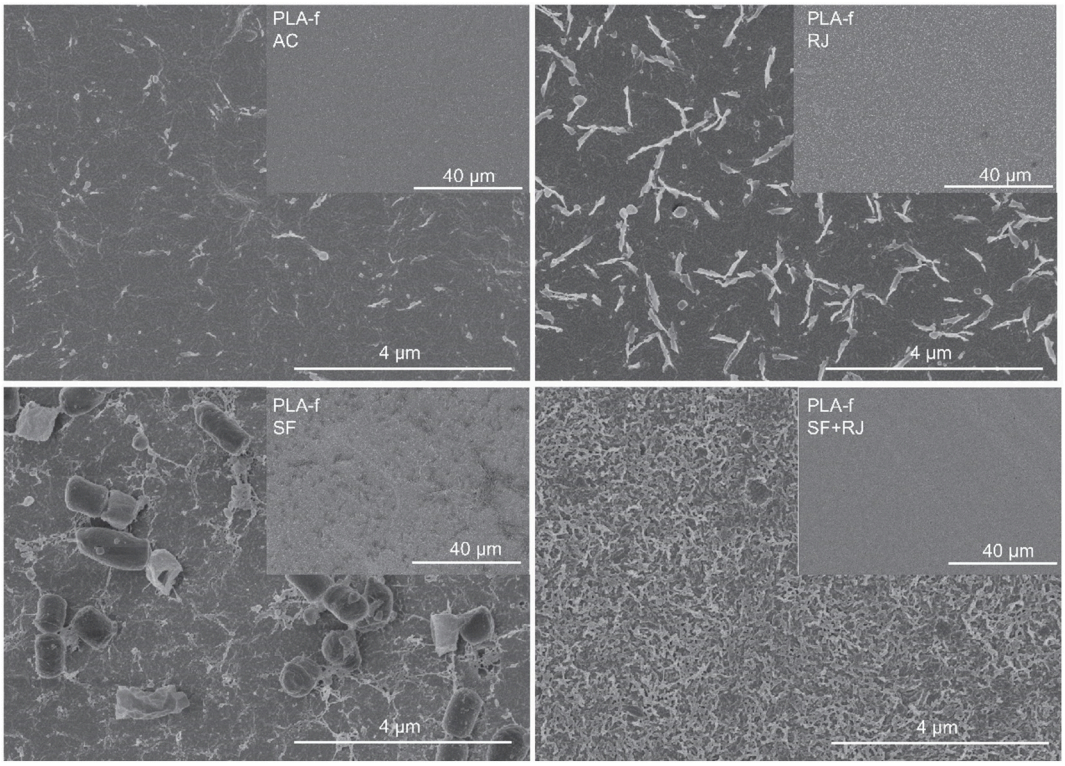

Fig. 4. Scanning electron microscope (SEM) images taken under 20,000× and 2000× (inset picture) magnifications exhibiting the surface morphology and colonization of different strains on PLA-f in 0.1× TSB liquid medium at 30 °C for 75 days. AC: abiotic control; RJ: *R. jostii*; SF: *S. fulvissimus*. SF-RJ: a mixture of SF and RJ.

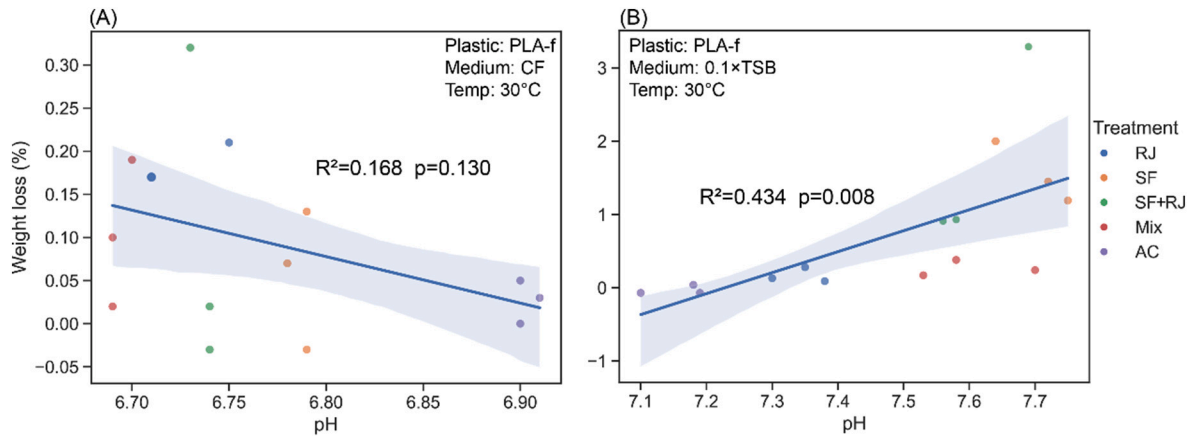

Fig. 5. Linear least-squares regression between the pH of culture media and the weight loss of PLA-f after 75 days of incubation in (A) carbon-free medium (CF) and (B) 0.1× tryptic soy broth medium (0.1 × TSB). The area above and below the fitting curve represents the 95 % confidence interval. AC: abiotic control; RJ: *R. jostii*; SF: *S. fulvissimus*; SF-RJ: a mixture of SF and RJ; Mix: a mixture of all 5 strains.

4. Discussion

4.1. LDPE-f, PBAT-f, Bionov-B and PLA-f degradation was not promoted under room temperature

4.1.1. No degradation in LDPE-f

In LDPE-f, no significant changes in weight loss and CI were observed among the treatments. That suggests no degradation for LDPE-f after 180 days of incubation. Interestingly, our outcomes diverge from a previous study reporting LDPE microplastics degradation facilitated by earthworm gut microbiome (Huerta Lwanga et al., 2018). In our case, utilizing the same strains of microorganisms did not yield noteworthy results. While this might appear contradictory, variations in experimental conditions likely contributed to these disparities. The prior study conducted degradation experiments at 20 °C in moist, sterile soils, utilizing a consortium of earthworm gut bacteria. They also employed LDPE microplastics that underwent aging and fragmentation at low temperatures, potentially rendering them more amenable to colonization. In addition, the techniques to assess and retrieve microplastics were not as advanced as we observe today, which may have led to the overestimation of LDPE degradation. Our study was conducted in a 0.1× TSB culture medium at room temperature (avg 19.4 °C), using LDPE macro-plastics rather than microplastics. This trend echoes the LDPE hard-wearing and non-degradable characteristics discussed in existing literature (van den Oever et al., 2017). These distinct experimental setups likely contributed to the divergence in findings regarding LDPE degradation. Considering these discrepancies, future investigations should consider these varying factors to unravel the underlying mechanisms of potential LDPE degradation.

4.1.2. PBAT-f and Bionov-B neglectable degradation

PBAT-f weight loss detected after 180 days was neglectable for all treatments. Although SG shows a slightly improved performance than the other strains to promote PBAT-f degradation, the weight loss values are minimal compared to previous research (Cho et al., 2022; Jia et al., 2021; Tseng et al., 2023). We should bear in mind that even though the lower temperatures ($\bar{x}$ =19.4 °C) mimicking environmental temperatures were neither optimal for PBAT-f degradation nor bacterial growth in Experiment 1, our aim with Experiment 1 was to understand how the chosen strains would behave under such conditions.

PBAT-f samples have not gone through notable changes in the molecular weight and crystallinity (Fig. 2 & Table 2), and the spectra of the sample subjected to SG did not show changes in chemical composition (Fig. S8).

Regarding the Bionov-B, weight loss did not differ among the treatments after 180-day incubation (Fig. 1C). Although SG seems to be triggering more weight loss of Bionov-B than other treatments, our data does not suffice for such a statement either after 90 or 180 days. Even though certain studies pointed out that PBAT film degradation stood out when compared to PBAT/PLA blends (Weng et al., 2013), several factors may have contributed to the inconspicuous statistical significance shown in Fig. 1C. The starch in the mulch films could have degraded at the early stage, as reported by a previous study using biodegradable seedling trays made of starch and PBAT/PLA blends (Meng et al., 2023a). Although the exact composition of additives in Bionov-B was not available, the commercial mulch film Bionov-B inevitably contains certain additives. It is, therefore, highly possible that the significant amount of leachates released from the mulch film are coming from additives and/or plastic-derived compounds (Serrano-Ruíz et al., 2020; Uzamurera et al., 2023), a fact that could have contributed to weight loss even without the presence of test strains. While these ideas provide insights, the mechanisms and complex factors driving Bionov-B degradation need further clarification.

4.1.3. PLA-f property changes and the need for in-depth assessment

Although PLA-f treated with SF for 180 days did not show substantial mass reduction, a reduction in molecular weight (M_n, M_w, M_z) was observed compared to the pristine film and AC (Fig. 2B), a reduction not seen for AC and RJ treatments. SF treatment, therefore, stands out even under unfavorable conditions for biodegradation, highlighting the potential to facilitate the onset of PLA bulk erosion (Fig. 6A), characterized by minor changes in the material mass and a decrease in the molecular weight (Burkersroda et al., 2002).

Experiment 1 was carried out at a temperature neither optimal for SF growth nor PLA degradation, which may pose a hurdle to emphatically stating that SF is a promising strain for PLA degradation. However, SF potential for degrading synthetic polymers is already widely reported (Rodríguez-Fonseca et al., 2021), e.g., Yottakot and Leelavatcharamas (2019) stated that SF amplified PLA weight loss by 30 folds when adjusting the PLA degradation conditions. Therefore, Experiment 2 was designed to clear this hurdle and enhance our understanding of how SF, isolated from the earthworm gut, would perform as a bioremediating agent under environmental soil temperatures.

Yet in Experiment 1, PLA-f samples treated with SF denoted increased crystallinity compared to the AC and the pristine film (both were completely amorphous). It is also noteworthy that one PLA-f disk in one of the replicate tubes in the SF treatment fragmented into two pieces after 75 days, and all PLA-f disks subjected to the SF treatment underwent a color change from transparent to white (Fig. S18), following the cleaning and drying procedures. Interestingly, the occurrence of

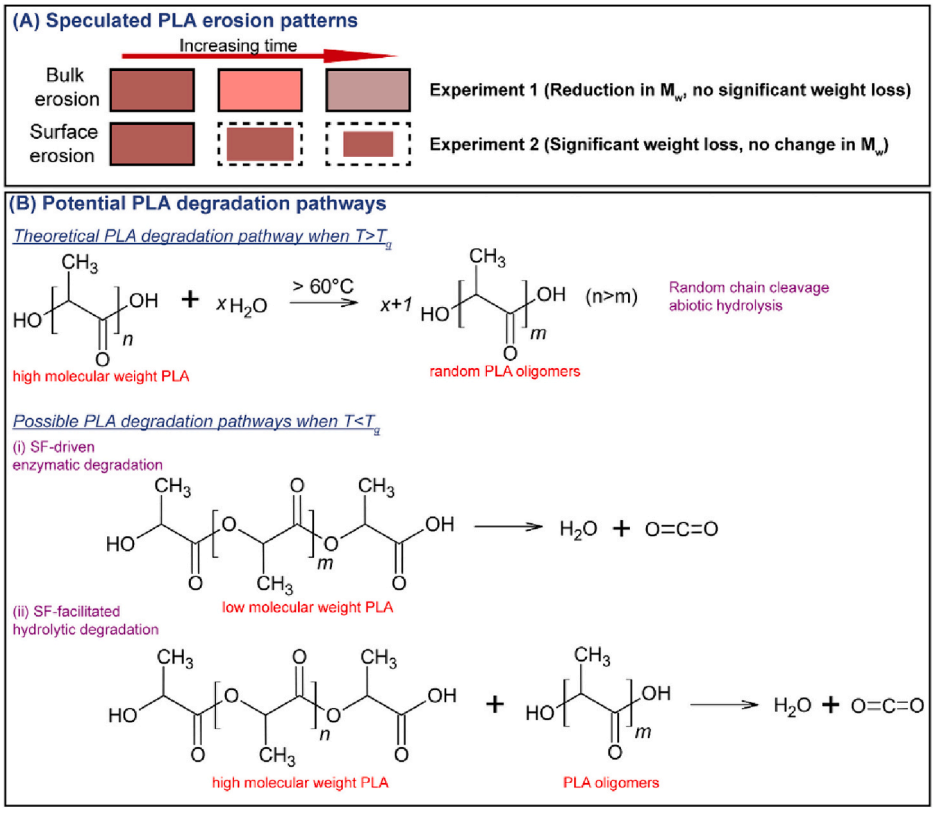

Fig. 6. (A) Schematic illustration of speculated PLA erosion patterns in different experiments. (B) Theoretical PLA degradation pathway when the temperature is above T_g, and possible PLA degradation pathways associated with SF when the temperature is under T_g. SF: *S. fulvissimus*. Where: Mw is weight-averaged molecular weight; T_g is PLA glass transition temperature, and *x* stands for the number of water molecules.

whiteness, specifically after the cleaning procedure, introduces an intriguing perspective. This occurrence suggests that crystallization might not solely be attributed to SF exposure. A study has revealed that PLA hydrolysis becomes evident when PLA samples are immersed in a low-concentration ethanol-water solution, inducing PLA crystallization (Yottakot and Leelavatcharamas, 2019). Considering that the whiteness only occurred in SF, while PLA-f disks in AC and RJ were processed in the same way, we speculate that the SF treatment might have rendered PLA-f more susceptible to crystallization. That could have been triggered by ethanol and drying, leading to increased crystallinity. Combining the weight loss, reduction in molecular weight, a changed tendency to crystallization, and the changes in color and brittleness, SF showed potential to facilitate the biodegradation of PLA-f, and its performance under 30 °C is discussed in Section 4.2.1.

4.2. Role of environmental factors in PLA degradation

4.2.1. Temperature

In Experiment 2, a higher temperature (30 °C) and the presence of TSB media shed light on more preeminent weight losses in PLA-f incubated with SF and SF + RJ (Fig. 1E). Such contrast may indicate that a higher temperature can promote SF growth and its key enzyme activity, thus optimizing PLA degradation (Al-Dhabi et al., 2019; Liao et al., 2009).

PLA-f molecular weight differed between the two experiments. In Experiment 1, only PLA-f from the SF treatment showed a lower molecular weight than the pristine material (Fig. 2B). However, PLA-f samples from both AC and SF treatment in Experiment 2 had a lighter molecular weight than their initial state in Experiment 1 (Fig. 2B, C). Besides, the PLA-f molecular weight exposed to SF was even lighter in Experiment 2 than in Experiment 1, even though the exposure time in Experiment 2 was almost half of the Experiment 1 duration. Both comparisons provide evidence that a higher temperature can facilitate PLA degradation in terms of its chemical properties, although below PLA T_g. Similar findings were also reported by Lunt (1998), where an increase in temperature from 13 °C to 30 °C shortened the onset of PLA fragmentation and biodegradation in aquatic systems by ~82 %. Hence, it can be inferred that the higher temperature facilitated PLA degradation and impacted its macromolecular structure by boosting the activity of SF enzymes. Also, the higher temperatures could have accelerated the process of PLA degradation, highlighted by the substantial reduction in PLA molecular weight after incubation. The latter proposition is corroborated by the accelerated breaking of PLA polymer chains with a higher temperature (Al-Dhabi et al., 2019).

4.2.2. Carbon source

Carbon from tryptone, soytone, and glucose in the TSB culture media may have contributed to more noticeable PLA-f weight loss in Experiment 2 compared to the lack of weight loss in CF media (Fig. 1E). The more preeminent weight losses when PLA-f was not the sole carbon source may indicate the importance of additional carbon sources to enable SF growth before interacting with PLA and perhaps assist in co-metabolizing PLA. Such findings were also reported in previous research where the addition of soytone, a media with high concentrations of carbohydrates and vitamins, promoted PLA bacterial degradation (Boonluksiri et al., 2021).

4.2.3. pH

After 180 days, the significantly lower pH observed for PLA-f, PBAT-f, and Bionov-B compared to LDPE-f in the AC treatment could indicate the hydrolysis of polyesters without the presence of microbes. In general, the presence of SF was always associated with higher pH in the final culture media and higher weight loss in PLA-f. Similarly, the presence of SG coincided with slightly higher pH and PBAT-f weight loss. It was

reported that the erosion mechanism of polymers can be either surface erosion or bulk erosion (Fig. 6A), depending on the conditions, e.g., pH (Burkersroda et al., 2002). However, under alkaline conditions, PLA might undergo immediate and linear mass reduction while the remaining molecular weight remains the same, resulting in a surface erosion pattern. While under neutral–acidic conditions, PLA might undergo bulk erosion where the mass reduction is minor before reaching a tipping point, but the molecular weight starts to decrease first.

We were not able to tell if the increased weight loss was caused by the active consumption of PLA by the microorganisms (e.g., SF) and the pH change might simply stem from the byproducts of biodegraded plastics and not necessarily dominate plastic degradation (Xu et al., 2011). Alternatively, the presence of microorganisms increased the media pH, making the environmental conditions more favorable for the hydrolysis of PLA. Nevertheless, considering these findings, PLA-f degradation could be optimized by raising the environmental pH, a base-catalyzed process supported by several studies (de Jong et al., 2001; Jia et al., 2021; Kanwal et al., 2022). Hence, future investigations could incorporate pH as a controlled variable to elucidate the potential mechanism underlying the positive correlation between pH and plastic degradation.

PLA degradation can occur by hydrolytic degradation of the ester groups in acid-catalyzed, base-catalyzed, and uncatalyzed media. Its kinetic constant normalized with pH shows that hydrolysis is more preeminent between acidic pH ranging from 1 to 3 and then gradually enhances the more basic the pH becomes from 6 to 10 (Gorrasi and Pantani, 2018). The slight basic pH observed in our PLA-f exposed to SF in TSB media suggests the cleavage of backbone esters and the lactide formation at higher pH instead of chain-end scission. Since the pH did not drop to acidic, we could not infer that the ester bonds were catalyzed by protons and terminal esters instead of the backbone esters (de Jong et al., 2001). Nevertheless, the backbiting mechanism leading to the lactide formation can also be observed at higher pH (van Nostrum et al., 2004).

4.2.4. Plastic surface colonization

Since AC control showed no biofilm formation and PLA-f incubated with SF + RJ had the densest biofilm, followed by the one in the SF and RJ treatments, the qualitative SEM images may serve as additional evidence to infer that the ongoing biodegradation of PLA-f may be associated with the corresponding bacterial strains.

4.2.5. Possible degradation pathways for PLA-f

SF potential to facilitate PLA-f degradation in temperatures under PLA glass transition temperature (T_g ~ 55–60 °C) is one of the major novelties of this study. PLA degradation rate is minimal at ambient temperatures due to the lower hydrolytic degradation in temperatures under PLA T_g (Rosli et al., 2021). Hence, the observed gravimetric and molecular loss of PLA-f exposed to SF highlights the strain's potential to facilitate alternative paths to abiotic hydrolytic degradation. SF may have facilitated PLA-f degradation by enzymatic hydrolysis or, less likely, oxidation. SF enzymatic shortcut to tackle PLA-f even under its T_g could be explained by the extracellular hydrolases and/or depolymerase-like enzymes produced by SF (Mihajlovski et al., 2021).

Fig. 6B shows the possible plastic degradation pathways optimized by the SF inoculation compared to the standard hydrolytic degradation occurring with PLA when the tested temperature is above the PLA T_g. When the tested temperature is below T_g, the PLA degradation is reported as marginal (Gorrasi and Pantani, 2018). However, when the temperature is higher than T_g or microbial organisms accelerate the process, PLA degradation tends to occur mainly in the bulk of the material. After chain scission, the PLA molecule is broken into lactic acid oligomers, increasing carboxylic acid end groups. Hence, such group availability accelerates PLA degradation even further, initiating a self-catalyzed and self-maintained process (Vert, 2005).

Although high-molecular weight PLA (>20 kDa) tends to show resistance to microbial attacks (Rosli et al., 2021), the reported decrease in molecular weight when comparing the pristine PLA-f from >100 kDa to <100 kDa after exposure to SF suggests SF as a facilitator of PLA marginal degradation at mesophilic temperatures. The formation of lactide by the intratransesterification reactions (Ozdemir and Hacaloglu, 2016) mainly occurs after the diffusion of water into the material, followed by hydrolysis of chains in PLA amorphous regions. That leads to decreased molecular weight and hydrolysis of the lamellae of crystalline regions, resulting from the autocatalytic mechanisms by the acidic degradation products and higher concentration of carboxylic acid at chain ends (Metters et al., 2000; Tokiwa and Calabia, 2006).

4.3. Prospects and challenges of plastic degradation driven by bacteria isolated from the earthworm gut

4.3.1. Efficiency of bacterial degradation

The findings in this study have pointed out that bacteria isolated from the earthworm gut, mainly SF, show the potential for optimizing PLA-f degradation. Although the degrading rate is limited in our experimental setup, many degradation proxies have reached a statistical significance level ($p < 0.05$). This study does not intend to infer complete plastic degradation but enhance our fundamental understanding of how the earthworm gut microorganisms tackle or not different types of plastics. Further in-depth studies testing factors, such as environmental temperature and nutrient source, can be conducted to optimize our understanding and methodological setup. At the same time, additional experiments and soil incubations should be considered to examine if such bacterial degradation can be efficient enough to be implemented as a bioremediation strategy in the field.

4.3.2. Feasibility of bacterial degradation

In this study, SEM images brought to light that different polymers incubated on the same TSB solid culture media with SF presented distinct biofilms. Biofilms were only formed on the surface of PLA-f, PBAT-f, and Bionov-B, while the LDPE-f surface remained neat without biofilm (Fig. 3). That suggests SF struggles to colonize LDPE-f films effectively. These outcomes can be attributed to the inherent hydrophobic properties of both the bacteria and the plastics. Previous studies revealed that PLA generally possesses more hydrophilicity than PBAT (Zheng et al., 2023), followed by LDPE (Ganesan et al., 2022). Hence, PLA-f, PBAT-f, and the Bionov-B tend to exhibit higher hydrophilicity than LDPE-f. In this scenario, the SF vegetative hyphae and their hydrophilic characteristics may lead to a greater propensity to colonize those plastic surfaces instead of LDPE-f ones (Zambri et al., 2022). That reflects the polymer-specific feature of a potential plastic-degrading strain. On the other hand, by profiling the colonization of different strains on the same plastic (PLA-f, Fig. 4) and comparing the biofilm formation with weight loss achieved (Fig. 1E), it was also clear that the potential of a plastic-degrading strain might be limited to its accessibility to the polymer. The interplay between different strains in the same system could also affect the efficacy of biodegradation. The co-existence of SF and RJ led to better biofilm formation (Fig. 4) than SF or RJ alone, and the PLA weight loss in SF + RJ was also higher despite the variance (Fig. 1E). That could indicate a good mutualism between SF and RJ, magnifying the plastic degradation potential. While the co-existence of all strains in the system led to lower weight loss than SF alone or SF + RJ, this could indicate what happens in the real-world scenario where "plastic degraders" may face competition and unfavorable situations to strive and multiply within the soil microbial community. The feasibility of microorganisms-driven plastic biodegradation in soil systems may be improved by introducing fungi that have also shown the potential to optimize plastic degradation (Srikanth et al., 2022; Wu et al., 2023).

Although our study did not follow techniques recommended to quantify the conversion of plastic's carbon into CO_2 to assess biodegradation (Zumstein et al., 2019), other refined techniques, such as GPC,

DSC, SEM, and ATR-FTIR, were employed to corroborate the weight loss and further characterize the degradation of the remaining plastic in the system. That represents a viable and cost-efficient alternative to enhance our exploratory understanding of plastic degradation. Testing the microorganisms' potential as plastic degraders only in liquid media may appear as a study limitation; however, our experiments were thought to investigate and understand their biodegrading potential in a controlled system. Further experiments are needed to comprehend how these earthworm gut-isolated microorganisms interact with plastics in both controlled and open systems. Then, a thorough assessment in different soils, combining different bacterial strains, should be carried out to comprehend the potential of such microorganisms to optimize plastic degradation in the environment.

5. Conclusion

The current study explored the potential of bacterial strains isolated from earthworm gut to degrade plastics commonly used to produce mulch films for agricultural applications. We revealed that (1) at room temperature ($\bar{x}$ =19.4 °C), the weight losses of all tested plastics (LDPE-f, PLA-f, PBAT-f, and Bionov-B) were neglectable after 180 days incubated in the dark. Although the gravimetric weight loss of PLA-f was minimal, the presence of SF triggered a decreased molecular weight and increased crystallinity compared to its initial state. We explored PLA-f degradation at a higher temperature (30 °C), using different culture media and strain mixtures. We further found that (2) at 30 °C and in the presence of 0.1× TSB media, SF and SF + RJ treatments promoted the degradation of PLA-f (3). A positive correlation between weight loss and pH was found, which might reflect the degradation mechanisms of PLA. (4) The interplay of different strains in the same system could affect the performance of promising plastic degraders. After exploring the potential of bacterial strains isolated from *Lumbricus terrestris* on plastic degradation, SF stood out as a possible candidate to optimize PLA-f degradation even below PLA T_g. Further studies are needed to explore the feasibility of applying SF for longer periods in culture media and soils.

CRediT authorship contribution statement

Davi R. Munhoz: Writing – review & editing, Writing – original draft, Validation, Methodology, Investigation, Formal analysis, Data curation, Conceptualization, Visualization. **Ke Meng:** Writing – review & editing, Writing – original draft, Visualization, Validation, Methodology, Investigation, Formal analysis, Data curation, Conceptualization. **Lang Wang:** Writing – original draft, Investigation, Formal analysis, Data curation. **Esperanza Huerta Lwanga:** Writing – review & editing, Supervision, Funding acquisition. **Violette Geissen:** Writing – review & editing, Supervision, Project administration, Funding acquisition. **Paula Harkes:** Writing – review & editing, Supervision, Project administration, Funding acquisition.

Declaration of competing interest

The authors declare that they have no known competing financial interests or personal relationships that could have appeared to influence the work reported in this paper.

Data availability

Data will be made available on request.

Acknowledgement

This work was supported by the European Union's Horizon 2020 research and innovation programme under the Marie Skłodowska-Curie grant agreement [No 955334, 2020] and the China Scholarship Council [CSC: 201904910443]. We would like to thank Herman de Beukelaer for the DSC analysis, Wouter Teunissen for the GPC analysis, Marcel Giesbers and Jelmer Vroom for the SEM analysis, and NIOO for the frozen isolated bacteria. We also acknowledge Maarten van der Zee for his meticulous contribution to the results and discussion section.

Appendix A. Supplementary data

Supplementary data to this article can be found online at https://doi.org/10.1016/j.scitotenv.2024.172175.

References

Adhikari, K., Astner, A.F., DeBruyn, J.M., Yu, Y., Hayes, D.G., O'Callahan, B.T., Flury, M., 2023. Earthworms exposed to polyethylene and biodegradable microplastics in soil: microplastic characterization and microbial community analysis. ACS Agric. Sci. Technol. 3 (4), 340–349.

Al-Dhabi, N.A., Esmail, G.A., Duraipandiyan, V., Arasu, M.V., 2019. Chemical profiling of *Streptomyces sp. Al-Dhabi-2* recovered from an extreme environment in Saudi Arabia as a novel drug source for medical and industrial applications. Saudi J. Biol. Sci. 26 (4), 758–766. https://doi.org/10.1016/j.sjbs.2019.03.009.

Bonifer, K.S., Wen, X., Hasim, S., Phillips, E.K., Dunlap, R.N., Gann, E.R., DeBruyn, J.M., Reynolds, T.B., 2019. *Bacillus pumilus B12* degrades polylactic acid and degradation is affected by changing nutrient conditions [original research]. Front. Microbiol. 10. https://www.frontiersin.org/articles/10.3389/fmicb.2019.02548.

Boonluksiri, Y., Prapagdee, B., Sombatsompop, N., 2021. Promotion of polylactic acid biodegradation by a combined addition of PLA-degrading bacterium and nitrogen source under submerged and soil burial conditions. Polym. Degrad. Stab. 188, 109562 https://doi.org/10.1016/j.polymdegradstab.2021.109562.

Burkersroda, F.v., Schedl, L., Göpferich, A., 2002. Why degradable polymers undergo surface erosion or bulk erosion. Biomaterials 23 (21), 4221–4231. https://doi.org/10.1016/S0142-9612(02)00170-9.

Chamas, A., Moon, H., Zheng, J., Qiu, Y., Tabassum, T., Jang, J.H., Suh, S., 2020. Degradation rates of plastics in the environment. ACS Sustain. Chem. Eng. 8 (9), 3494–3511.

Chen, H.L., Nath, T.K., Chong, S., Foo, V., Gibbins, C., Lechner, A.M., 2021. The plastic waste problem in Malaysia: management, recycling and disposal of local and global plastic waste. SN Appl. Sci. 3 (4), 437. https://doi.org/10.1007/s42452-021-04234-y.

Cho, J.Y., Park, S.L., Kim, S.H., Jung, H.J., Cho, D.H., Kim, B.C., Bhatia, S.K., Gurav, R., Park, S.-H., Park, K., Yang, Y.-H., 2022. Novel poly(butylene adipate-co-terephthalate)-degrading *Bacillus sp. JY35* from wastewater sludge and its broad degradation of various bioplastics. Waste Manag. 144, 1–10. https://doi.org/10.1016/j.wasman.2022.03.003.

de Jong, S.J., Arias, E.R., Rijkers, D.T.S., van Nostrum, C.F., Kettenes-van den Bosch, J.J., Hennink, W.E., 2001. New insights into the hydrolytic degradation of poly(lactic acid): participation of the alcohol terminus. Polymer 42 (7), 2795–2802. https://doi.org/10.1016/S0032-3861(00)00646-7.

Ganesan, S., Ruendee, T., Kimura, S.Y., Chawengkijwanich, C., Janjaroen, D., 2022. Effect of biofilm formation on different types of plastic shopping bags: structural and physicochemical properties. Environ. Res. 206, 112542 https://doi.org/10.1016/j.envres.2021.112542.

Gorrasi, G., Pantani, R., 2018. Hydrolysis and biodegradation of poly(lactic acid). In: Di Lorenzo, M.L., Androsch, R. (Eds.), Synthesis, Structure and Properties of Poly(lactic acid). Springer International Publishing, pp. 119–151. https://doi.org/10.1007/12_2016_12.

Griffin-LaHue, D., Ghimire, S., Yu, Y., Scheenstra, E.J., Miles, C.A., Flury, M., 2022. In-field degradation of soil-biodegradable plastic mulch films in a Mediterranean climate. Sci. Total Environ. 806, 150238 https://doi.org/10.1016/j.scitotenv.2021.150238.

Han, Y., Teng, Y., Wang, X., Ren, W., Wang, X., Luo, Y., Zhang, H., Christie, P., 2021. Soil type driven change in microbial community affects poly(butylene adipate-co-terephthalate) degradation potential. Environ. Sci. Technol. 55 (8), 4648–4657. https://doi.org/10.1021/acs.est.0c04850.

Ho, K.-L.G., Pometto, A.L., Hinz, P.N., 1999. Effects of temperature and relative humidity on polylactic acid plastic degradation. J. Environ. Polym. Degrad. 7 (2), 83–92. https://doi.org/10.1023/A:1021808317416.

Huerta Lwanga, E., Thapa, B., Yang, X., Gertsen, H., Salánki, T., Geissen, V., Garbeva, P., 2018. Decay of low-density polyethylene by bacteria extracted from earthworm's guts: a potential for soil restoration. Sci. Total Environ. 624, 753–757. https://doi.org/10.1016/j.scitotenv.2017.12.144.

Jia, H., Zhang, M., Weng, Y., Zhao, Y., Li, C., Kanwal, A., 2021. Degradation of poly (butylene adipate-co-terephthalate) by *Stenotrophomonas sp. YCJ1* isolated from farmland soil. J. Environ. Sci. 103, 50–58. https://doi.org/10.1016/j.jes.2020.10.001.

Kanwal, A., Zhang, M., Sharaf, F., Chengtao, L., 2022. Screening and characterization of novel lipase producing Bacillus species from agricultural soil with high hydrolytic activity against PBAT poly (butylene adipate co terephthalate) co-polyesters. Polym. Bull. 79 (11), 10053–10076. https://doi.org/10.1007/s00289-021-03992-4.

Khalid, N., Aqeel, M., Noman, A., Rizvi, Z.F., 2023. Impact of plastic mulching as a major source of microplastics in agroecosystems. J. Hazard. Mater. 445, 130455.

Liao, Y., Wei, Z.-H., Bai, L., Deng, Z., Zhong, J.-J., 2009. Effect of fermentation temperature on validamycin A production by *Streptomyces hygroscopicus 5008*. J. Biotechnol. 142 (3), 271–274. https://doi.org/10.1016/j.jbiotec.2009.04.015.

Liu, E.K., He, W.Q., Yan, C.R., 2014. 'White revolution' to 'white pollution'—agricultural plastic film mulch in China. Environ. Res. Lett. 9 (9), 091001.

Lunt, J., 1998. Large-scale production, properties and commercial applications of polylactic acid polymers. Polym. Degrad. Stab. 59 (1), 145–152. https://doi.org/10.1016/S0141-3910(97)00148-1.

Maaskant, E., Aarsen, C.V., van Es, D.S., 2023. Accelerated weathering of furanoate polyesters: effect of molecular weight, crystallinity, and time. J. Appl. Polym. Sci. 140 (29), e54062.

Meng, K., Lwanga, E.H., van der Zee, M., Munhoz, D.R., Geissen, V., 2023a. Fragmentation and depolymerization of microplastics in the earthworm gut: a potential for microplastic bioremediation? J. Hazard. Mater. 447, 130765 https://doi.org/10.1016/j.jhazmat.2023.130765.

Meng, K., Teng, Y., Ren, W., Wang, B., Geissen, V., 2023b. Degradation of commercial biodegradable plastics and temporal dynamics of associated bacterial communities in soils: a microcosm study. Sci. Total Environ. 865, 161207 https://doi.org/10.1016/j.scitotenv.2022.161207.

Metters, A.T., Bowman, C.N., Anseth, K.S., 2000. A statistical kinetic model for the bulk degradation of PLA-b-PEG-b-PLA hydrogel networks. J. Phys. Chem. B 104 (30), 7043–7049. https://doi.org/10.1021/jp000523t.

Mihajlovski, K., Buntić, A., Milić, M., et al., 2021. From agricultural waste to biofuel: enzymatic potential of a bacterial isolate *Streptomyces fulvissimus CKS7* for bioethanol production. Waste Biomass Valor 12, 165–174. https://doi.org/10.1007/s12649-020-00960-3.

Ozdemir, E., Hacaloglu, J., 2016. Thermal degradation of polylactide and its electrospun fiber. Fibers Polym. 17, 66–73. https://doi.org/10.1007/s12221-016-5679-5.

Peng, B.-Y., Li, Y., Fan, R., Chen, Z., Chen, J., Brandon, A.M., Criddle, C.S., Zhang, Y., Wu, W.-M., 2020. Biodegradation of low-density polyethylene and polystyrene in superworms, larvae of *Zophobas atratus* (Coleoptera: Tenebrionidae): broad and limited extent depolymerization. Environ. Pollut. 266, 115206 https://doi.org/10.1016/j.envpol.2020.115206.

Rillig, M.C., Ingraffia, R., de Souza Machado, A.A., 2017. Microplastic incorporation into soil in agroecosystems [opinion]. Front. Plant Sci. 8 https://doi.org/10.3389/fpls.2017.01805.

Rillig, M.C., Lehmann, A., de Souza Machado, A.A., Yang, G., 2019. Microplastic effects on plants. New Phytol. 223 (3), 1066–1070. https://doi.org/10.1111/nph.15794.

Rodríguez-Fonseca, M.F., Sánchez-Suárez, J., Valero, M.F., Ruiz-Balaguera, S., Díaz, L.E., 2021. *Streptomyces* as potential synthetic polymer degraders: a systematic review. Bioengineering 8 (11).

Rosli, N.A., Karamanlioglu, M., Kargarzadeh, H., Ahmad, I., 2021. Comprehensive exploration of natural degradation of poly(lactic acid) blends in various degradation media: a review. Int. J. Biol. Macromol. 187, 732–741. https://doi.org/10.1016/j.ijbiomac.2021.07.196.

Sa'adu, I., Farsang, A., 2023. Plastic contamination in agricultural soils: a review. Environ. Sci. Eur. 35 (1), 13. https://doi.org/10.1186/s12302-023-00720-9.

Sander, M., 2019. Biodegradation of polymeric mulch films in agricultural soils: concepts, knowledge gaps, and future research directions. Environ. Sci. Technol. 53 (5), 2304–2315.

Serrano-Ruíz, H., Eras, J., Martín-Closas, L., Pelacho, A.M., 2020. Compounds released from unused biodegradable mulch materials after contact with water. Polym. Degrad. Stab. 178, 109202 https://doi.org/10.1016/j.polymdegradstab.2020.109202.

Sintim, H.Y., Bary, A.I., Hayes, D.G., Wadsworth, L.C., Anunciado, M.B., English, M.E., Bandopadhyay, S., Schaeffer, S.M., DeBruyn, J.M., Miles, C.A., Reganold, J.P., Flury, M., 2020. In situ degradation of biodegradable plastic mulch films in compost and agricultural soils. Sci. Total Environ. 727, 138668 https://doi.org/10.1016/j.scitotenv.2020.138668.

Srikanth, M., Sandeep, T.S.R.S., Sucharitha, K., et al., 2022. Biodegradation of plastic polymers by fungi: a brief review. Bioresour. Bioprocess. 9, 42. https://doi.org/10.1186/s40643-022-00532-4.

Tokiwa, Y., Calabia, B.P., 2006. Biodegradability and biodegradation of poly(lactide). Appl. Microbiol. Biotechnol. 72 (2), 244–251. https://doi.org/10.1007/s00253-006-0488-1.

Tseng, W.-S., Lee, M.-J., Wu, J.-A., Kuo, S.-L., Chang, S.-L., Huang, S.-J., Liu, C.-T., 2023. Poly(butylene adipate-co-terephthalate) biodegradation by *Purpureocillium lilacinum strain BA1S*. Appl. Microbiol. Biotechnol. 107 (19), 6057–6070. https://doi.org/10.1007/s00253-023-12704-z.

Tsou, C.-H., Chen, Z.-J., Yuan, S., Ma, Z.-L., Wu, C.-S., Yang, T., Jia, C.-F., Reyes De Guzman, M., 2022. The preparation and performance of poly(butylene adipate) terephthalate/corn stalk composites. Curr. Res. Green Sustain. Chem. 5, 100329 https://doi.org/10.1016/j.crgsc.2022.100329.

Uzamurera, A.G., Wang, P.Y., Zhao, Z.Y., Tao, X.P., Zhou, R., Wang, W.Y., Xiong, Y.C., 2023. Thickness-dependent release of microplastics and phthalic acid esters from polythene and biodegradable residual films in agricultural soils and its related productivity effects. J. Hazard. Mater. 448, 130897.

van den Oever, M., Molenveld, K., van der Zee, M., Bos, H., 2017. Bio-based and Biodegradable Plastics: Facts and Figures: Focus on Food Packaging in the Netherlands. (Wageningen Food & Biobased Research; No. 1722). Wageningen Food & Biobased Research. https://doi.org/10.18174/408350.

van Nostrum, C.F., Veldhuis, T.F.J., Bos, G.W., Hennink, W.E., 2004. Hydrolytic degradation of oligo(lactic acid): a kinetic and mechanistic study. Polymer 45 (20), 6779–6787. https://doi.org/10.1016/j.polymer.2004.08.001.

Vert, M., 2005. Polyglycolide and copolyesters with lactide. In: Steinbüchel, A. (Ed.), Biopolymers Online. https://doi.org/10.1002/3527600035.bpol4006.

Wang, Y., Hu, T., Zhang, W., Lin, J., Wang, Z., Lyu, S., Tong, H., 2023. Biodegradation of polylactic acid by a mesophilic bacteria *Bacillus safensis*. Chemosphere 318, 137991. https://doi.org/10.1016/j.chemosphere.2023.137991.

Weng, Y.-X., Jin, Y.-J., Meng, Q.-Y., Wang, L., Zhang, M., Wang, Y.-Z., 2013. Biodegradation behavior of poly(butylene adipate-co-terephthalate) (PBAT), poly (lactic acid) (PLA), and their blend under soil conditions. Polym. Test. 32 (5), 918–926. https://doi.org/10.1016/j.polymertesting.2013.05.001.

Wu, F., Guo, Z., Cui, K., Dong, D., Yang, X., Li, J., Wu, Z., Li, L., Dai, Y., Pan, T., 2023. Insights into characteristics of white rot fungus during environmental plastics adhesion and degradation mechanism of plastics. J. Hazard. Mater. 448, 130878 https://doi.org/10.1016/j.jhazmat.2023.130878.

Wufuer, R., Li, W., Wang, S., Duo, J., 2022. Isolation and degradation characteristics of PBAT film degrading bacteria. Int. J. Environ. Res. Public Health 19 (24).

Xu, L., Crawford, K., Gorman, C.B., 2011. Effects of temperature and pH on the degradation of poly(lactic acid) brushes. Macromolecules 44 (12), 4777–4782. https://doi.org/10.1021/ma2000948.

Yang, J., Yang, Y., Wu, W.M., Zhao, J., Jiang, L., 2014. Evidence of polyethylene biodegradation by bacterial strains from the guts of plastic-eating waxworms. Environ. Sci. Technol. 48 (23), 13776–13784.

Yoshida, S., Hiraga, K., Takehana, T., Taniguchi, I., Yamaji, H., Maeda, Y., Oda, K., 2016. A bacterium that degrades and assimilates poly (ethylene terephthalate). Science 351 (6278), 1196–1199.

Yottakot, S., Leelavatcharamas, V., 2019. Isolation and optimisation of polylactic acid (PLA)-packaging-degrading actinomycete for PLA-packaging degradation. Pertanika J. Trop. Agric. Sci. 42 (3).

Zambri, M.P., Williams, M.A., Elliot, M.A., 2022. Chapter five - how Streptomyces thrive: advancing our understanding of classical development and uncovering new behaviors. In: Poole, R.K., Kelly, D.J. (Eds.), Advances in Microbial Physiology, Vol. 80. Academic Press, pp. 203–236. https://doi.org/10.1016/bs.ampbs.2022.01.004.

Zhang, C., Lan, Q., Zhai, T., Nie, S., Luo, J., Yan, W., 2018. Melt crystallization behavior and crystalline morphology of polylactide/poly (ε-caprolactone) blends compatibilized by lactide-caprolactone copolymer. Polymers 10 (11), 1181.

Zheng, Y., Jia, X., Zhao, Z., Ran, Y., Du, M., Ji, H., Pan, Y., Li, Z., Ma, X., Liu, Y., Duan, L., Li, X., 2023. Innovative natural antimicrobial natamycin incorporated titanium dioxide (nano-TiO2)/poly (butylene adipate-co-terephthalate) (PBAT)/poly (lactic acid) (PLA) biodegradable active film (NTP@PLA) and application in grape preservation. Food Chem. 400, 134100 https://doi.org/10.1016/j.foodchem.2022.134100.

Zumstein, M.T., Narayan, R., Kohler, H.-P.E., McNeill, K., Sander, M., 2019. Dos and do nots when assessing the biodegradation of plastics. Environ. Sci. Technol. 53 (17), 9967–9969. https://doi.org/10.1021/acs.est.9b04513.